RSC Advances

ROYAL SOCIETY OF CHEMISTRY

www.rsc.org/advances

Journal Name

RSCPublishing

ARTICLE

Easy Extraction of Water-soluble Graphene Quantum Dots for Light Emitting Diodes

Cite this: DOI: 10.1039/xoxxooooox

Gundam Sandeep Kumar, Umamahesh Thupakula, Piyush Kanti Sarkar and Somobrata Acharya*

Received ooth January 2012,
Accepted ooth January 2012

DOI: 10.1039/xoxxooooox

www.rsc.org/

Graphene quantum dots (GQDs) have attracted numerous attentions due to their unique optoelectronic properties, which arise from quantum confinement effect or edge effect or surface functionalization. Popular routes of designing GQDs are based on the reactions in aqueous phases, which is detrimental for integration of GQDs into optoelectronic devices. Hence, a critical challenge remains in utilizing the water-soluble GQDs for fabricating optoelectronic devices. Here we demonstrate for the first time a single step facile route to extract water-soluble GQDs into solid powder under reduced pressure for the fabrication of light emitting diodes (LEDs). The process avoids the need of post synthesis ex-situ functionalization or the use of additional polymers to make GQDs hydrophobic retaining the intrinsic luminescent behavior of GQDs. The measured current-voltage characteristics of GQD-LED devices showed a significantly low turn-on voltage of ~ 2.5 V. A bias dependent electroluminescence leading to color tunability from blue to deep cyan is demonstrated.

Introduction

Graphene is at the centre of materials research owing to its unique perspective for a numerous applications for optoelectronics.[1-5] Pristine graphene is a zero band-gap material with an infinite exciton Bohr radius implying that the quantum confinement could take effect for any finite size of graphene.[6] The band-gap of graphene can be created by fabricating graphene nanoribbons (GNRs),[7] graphene quantum dots (GQDs)[8] or by means of chemical or physical treatments to alter the electronic structure.[9,10] Such modification leads to the tunable photoluminescence (PL) in graphene nanostructures making it potential material for optoelectronics.[11,12] GQDs are composed of a regular hexagonal lattice of sp^2 carbon atoms edged with some different atomic functional groups.[12] GQDs have attracted numerous attentions in optoelectronics, which arises from the quantum confinement effect,[9,13] edge effect,[10] and due to surface functionalization.[11] A wide range of tunable PL in the visible region is observed in case of GQDs with finite PL quantum yield (QY).[14-16] Tunable coloric properties and moderate QYs of GQDs are beneficial for lighting device fabrications.[11,12] Various approaches have been reported to synthesize GQDs such as glucose-derived water-soluble GQDs by hydrothermal method,[14] electrochemical synthesis,[15] hydrothermal graphene oxide reduction,[16] solvothermal method,[9] acid treatment of carbon fibres,[17] ammonia-mediated cutting of graphene oxide sheets into GQDs,[11,12] and MBEs[18]. A popular route in preparing GQDs is the Hummer's method to derive graphene oxide from graphite powder, followed by hydrothermal treatment in the presence of heteroatomic functional group materials.[10,11,16,19-22] However, most of these approaches are based on reactions in aqueous phases, which leads to poor solubility in common organic solvents limiting the use of solution process technologies for integration of GQDs into optoelectronic devices. Attempt to design "hydrophobic" GQDs involved ex-situ functionalization of surfaces, blending the GQDs with polymer,[21] GQDs-agar composites[23] or by amidative cutting of tattered graphite powder.[12] However, such routes to extract water-soluble GQDs to make compatible with organic solvents (modifying the medium of dispersion) for device fabrication affects the luminescence behavior of the as-prepared GQDs.[21] Since most of the reports for fabricating GQDs are based on aqueous phases, it is essential to develop a facile approach to extract water-soluble GQDs for thin film based optoelectronic device fabrication without disturbing the intrinsic character of as-prepared GQDs. Here we show that water-soluble GQDs can be used to fabricate electroluminescence (EL) devices without using additional polymers or further ex-situ functionalization. Simple evaporation process under reduced pressure using rotary evaporator system yields powder-GQDs, which are used for EL device fabrication. The intrinsic optical behavior of the powder-GQDs remains unaltered in comparison to the water-soluble GQDs suggesting retention of electronic properties in solid phase. Both the water-soluble and powder-GQDs show color tunable PL. We demonstrate the fabrication of color tunable light emitting diodes (LEDs) using GQDs as active layers. The devices show significantly low turn-on voltages of ~ 2.5 V at

ambient conditions. The successful demonstration on the fabrication of GQD-LED devices from the water-soluble GQDs may be found important towards using the water-soluble GQDs in optoelectronic applications.

Experimental section

Initially the graphene oxide sheets (GOS) were synthesized from the graphite powder by employing a well-known modified Hummers' method.[11,24] The GQDs were synthesized from GOSs by a simple one step hydrothermal process. In brief, for GQDs synthesis, 5 ml of GO solution (1 mg/1 ml loading), 5 ml of de-ionized (DI) water, and 3 ml of ammonia solutions were added together and subjected to hydrothermal reaction. The resultant solution was filtered through different pore size filter paper and ultrafiltration device to collect the GQDs for further characterization (see Supplementary Information for synthesis and characterization details).

Results and discussion

Transmission electron microscopy (TEM) image shows GQDs with diameters of 5 ± 0.5 nm (Figure 1a). The high resolution TEM (HRTEM) image (Figure 1b) indicates that the GQDs are highly crystalline with lattice spacing's of 0.24 ± 0.02 nm corresponding to hexagonal lattice fringes of graphene.[19] Corresponding Fast Fourier Transform (FFT) pattern clearly shows hexagonal pattern of the graphene structure corresponding to the (100) plane (Figure 1c). Graphene is a monolayer of carbon atoms arranged in a honeycomb lattice consisting of two equivalent triangular carbon sublattices A and B.[25] A single layer graphene shows six carbon atoms in hexagonal pattern in TEM images,[10] while triangular pattern can be viewed in few-layer graphene.[26] A highly resolved HRTEM image of the GQD (Figure 1d) reveals individual atoms of GQDs, which are denoted with green color dots. The HRTEM image shows the triangular sublattice pattern (AAA position) of carbon atoms instead of hexagonal ring pattern (ABABAB) of graphene. Imaging the individual atoms and measuring their positions involves the reconstruction of the wave-function of the imaging electron-wave field at the exit plane of the specimen,[27] and different number of layer gives rise to distinct interference patterns.[26] Hence, the GQDs consist of multiple graphene layers since the HR-TEM image shows the triangular pattern instead of hexagonal ring pattern.

The UV-vis spectrum of GQDs exhibits the two broad peaks at ~ 330 nm and ~ 420 nm, which are assigned to π - π* transition of C=C bonds and π - n transition of amino functionalization respectively (Figure 2a).[28-30] The broad nature of the UV-vis spectrum is attributed to the presence of additional closely packed energy levels, which may arise due to the amino functionalization.[28,30] The PL spectrum shows two prominent peaks at ~ 430 nm (blue emission) and ~ 490 nm (green emission) respectively when excited at ~ 340 nm (Figure 2b). The PL peaks are attributed to the intrinsic and defect (surface) state emission of GQDs respectively.[12,28,30,31] We have observed an effective emission from blue to cyan to green under variable excitations (Figure 2b). In fact, excitation dependent change of the intrinsic and defect PL positions for GQDs was reported earlier.[30] The color tunable PL from GQDs was observed through variation of pH or the solvent medium.[9] The surface functionalization of GQDs with pyrrole ring at edge sites induces the surface emissive defect states and

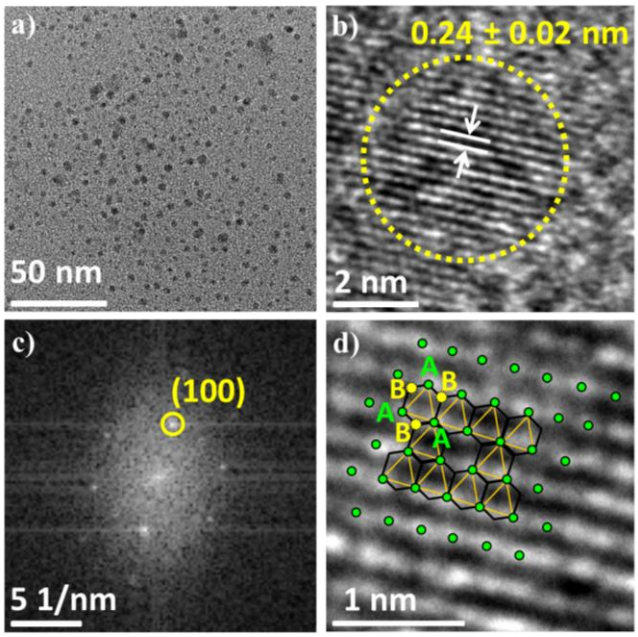

Figure 1. a) TEM image of GQDs showing uniform size distribution of ~ 5 ± 0.5 nm. b) HRTEM image of GQD. c) FFT pattern of corresponding GQD showing the six spots of hexagonal lattice belonging to (100) plane. d) Highly resolved HRTEM image showing the atomic view of GQD and the triangular sublattices A and B characteristic view of few layer graphene. The resolved carbon atoms are represented with green dot for sublattice A and yellow dots are for sublattice B to form the hexagonal ring of graphene.

enables the excitation dependent PL.[32] Recently, different mechanisms are considered for possible PL mechanisms in fluorescent carbon dots including GQDs, carbon nanodots and polymer dots.[31] Surface passivation of GQDs by amino functional groups replaces the non-radiative oxygenated moieties enabling the radiative recombination centres and color tunable PL.[11,19] Noteworthy, the intensity of ~ 490 nm peak becomes stronger upon changing the excitation from ~ 340 nm to ~ 420 nm, while the intensity of ~ 430 nm peak gradually decreases to disappear. However, both the peak positions remain the same upon changing the excitation energies. These excitation dependent PL results reveal that the excitation energy affects the PL properties of GQDs (Figure 2b). The peak at ~ 430 nm disappears probably because the excitation energy is not sufficient to excite the charge carriers to the π - π* transition.[28] The amino mediated PL peak at ~ 490 nm is observable in PL spectra beyond the ~ 400 nm excitation wavelength, as expected. Nevertheless, the PL wavelengths from the GQDs are tunable depending upon the excitation energy, which results in tunable PL from blue, cyan to green in water-soluble GQDs.

As prepared water-soluble GQDs exhibit highly luminescent behavior. The PL QY calculated with quinine sulphate as a reference (54% in 0.1 M H_2SO_4) is found to be ~ 28%, which matches well with the previous report.[11] The photoluminescence excitation (PLE) spectrum measured at the PL wavelength of ~ 430 nm shows a peak at ~ 370 nm while the PLE spectrum by monitoring ~ 490 nm PL peak shows strong peak at ~ 420 nm (Figure 2a). The PLE spectra reflect that luminescence from the GQDs have different origins.

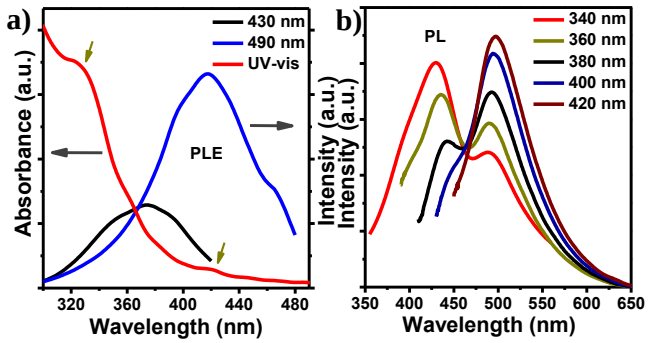

Figure 2. a) UV-vis and PLE spectra of as synthesized water-soluble GQDs. The emission wavelengths are shown in the inset. b) Excitation wavelength dependent PL spectra of as prepared water-soluble GQDs. The excitation wavelengths are shown in the inset.

Interestingly, the peak at ~ 370 nm overlaps with the intrinsic PL of GQDs suggesting a band-to-band transition for the intrinsic emission. The PLE spectra of GQDs with variable PL energy show a gradual change in the intensity indicating the existence of band tail by defect states (Figure 3a).[29] However, the prominent peaks in PLE spectra were not observed in the absorption spectrum, indicating that energy levels are closely spaced in GQDs causing broad absorption spectrum.

We have studied the recombination dynamics of water-soluble GQDs by performing the PL time decay measurements by varying the emission wavelengths (Figure 3b). A tri-exponential decay curve with fast (~ 6.6 ns) and slower (~ 8.1 ns) decay components corresponding to emission peaks at ~ 430 nm and ~ 490 nm respectively was observed. The defect state emission shows longer recombination lifetime compared to the intrinsic states.[28,29] A change in the radiative decay times and the PL peak positions strongly indicates the existence of different radiative recombination pathways in the GQDs. In general, the relaxation process is faster in case of emission related to high energy phonons.[28] Hence, with the high excitation energy of ~ 340 nm, the intrinsic emission peak at ~ 430 nm is dominated resulting in blue emission. When the excitation energy is lowered, the recombination occurs through the defect channels resulting in green emission at ~ 490 nm. However, at intermediate excitation wavelengths of ~ 360-380 nm, both the recombination channels have the equal probability resulting in cyan emission. The particular recombination channel in these transitions can be tuned or controlled by the excitation energy. As a result, the different radiative recombination channels result in tunable emission color from GQDs. These types of tunable emissive color materials are of importance for the optoelectronic applications.

We have employed a simple one step rotary evaporation technique to separate the GQDs from water phase (see Supplementary Information). The water from the GQDs sample was evaporated under reduced pressure of ~ 10^{-1} mbar at a temperature of ~ 45-55 °C to obtain powder-GQDs. The excitation wavelength dependent PL measurements are carried out for powder-GQDs (Figure 4a). The PL behavior of powder-GQDs is similar to the water-soluble GQDs with no significant change in the peak position. However, a significant change in the intensity of intrinsic to defect peak is observed. The defect peak is found to decrease with increase in the excitation

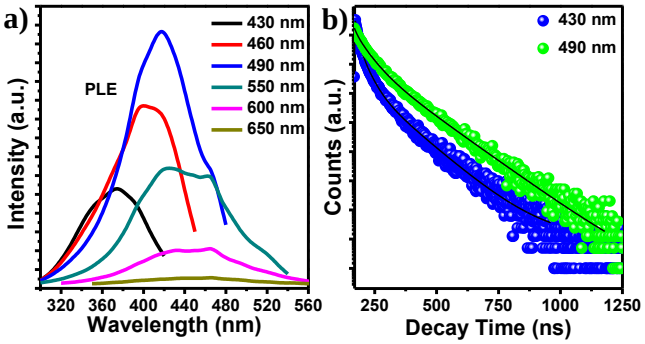

Figure 3. a) The PLE spectra of water-soluble GQDs with variable PL energy. The PL emission wavelengths are shown in the inset. b) The PL time decay profiles of water-soluble GQDs corresponding to intrinsic and defect state transitions as a function of emission wavelengths (Blue curve: excitation at 340 nm – emission at 430 nm and Green Curve: excitation at 410 nm – emission at 490 nm). The black lines specify the fitted curve while the scatter plots specify the experimental time decay profiles.

wavelengths. The PLE spectrum measured at the PL wavelength of ~ 430 nm show a peak at ~ 340 nm while the PLE spectrum by monitoring at ~ 490 nm shows a peak at ~ 370 nm showing a significant blue shift from the GQD-solution PLE (Figure 4b). The emissive traps on surface of GQDs created by the attachment of solvent molecules or ions or functional groups contributing to the defect state emission is highly susceptible to environment changes in solid state, which however is not affecting the intrinsic state emission. It appears that the surface passivating functional groups which induce non-radiative recombination of localized electron-hole pairs in solution medium is found to retain the intrinsic state emission in solid state. Thus the removal of solvent molecules makes intrinsic state emission play the leading role in PL behavior. True color photographic images of the water-soluble GQDs and powder-GQDs under UV-light source show high emission intensity (Figure 5a).

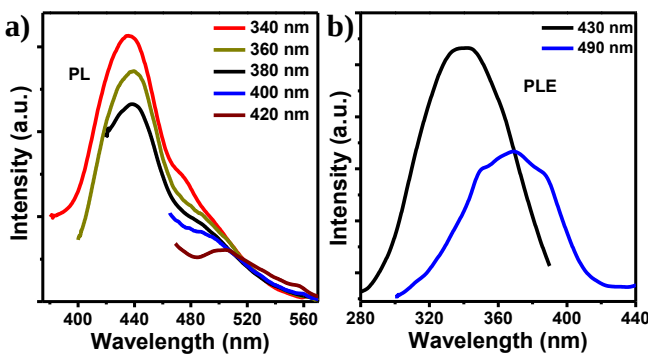

Figure 4. a) Excitation wavelength dependent PL spectra of powder-GQDs. The excitation wavelengths are shown in the inset. b) PLE spectra of powder-GQDs at different PL emission wavelengths. The emission wavelengths are shown in the inset.

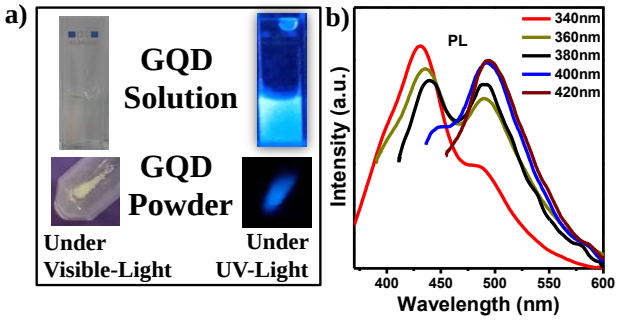

Figure 5. a) True color photographic images of as prepared water-soluble GQDs and powder-GQDs samples under visible light and UV-light source (365 nm). b) Excitation wavelength dependent PL spectra of powder-GQDs redispersed into water. The excitation wavelengths are shown in the inset.

In order to check the powder-GQDs retain the same intrinsic states in solid and solution phases, we have redispersed the powder-GQDs into water. The PL behavior is found to be similar to the as prepared water-soluble GQDs with no change in the peak position (Figure 5b). In addition, the observed suppression of PL peak intensity at ~ 490 nm in powder-GQDs is regained when the powder-GQDs are redispersed into water. This observation further reinforces the role of solvent molecules in the observed defect state emission of GQDs. Thus, the easy extraction process of powder-GQDs by rotary evaporation technique preserves the intrinsic properties of GQDs, which is beneficial for fabricating optoelectronic devices using GQDs. This is an important observation considering the large number of reports on water-soluble GQDs and the recent attempts to convert GQDs into "hydrophobic" for the possible optoelectronic applications.

We demonstrate fabrication of LEDs using powder-GQDs as active layer (see Supplementary Information). A schematic representation of the GQD-LED device is shown in Figure 6a. A thin layer of Poly (ethylene dioxythiophene) doped with polystyrene sulfonic acid (PEDOT:PSS) hole injection layer is deposited by spin-coating onto patterned indium tin oxide (ITO) coated glass substrates. On top of the PEDOT:PSS thin film, organic hole-transport layer poly-TPD is spin-coated. Subsequently, the dried powder-GQDs dissolved in ethanol are deposited on top of poly-TPD layer. The ZnO nanoparticles are used as electron injecting layer and spin coated on top of the GQDs layer. Finally, aluminum (Al) electrodes are thermally evaporated on the top of the ZnO layer. Corresponding energy band diagram (with respect to vacuum level) for layered structure GQD-LED device is shown in the inset of Figure 6a. The Fermi level of the GQDs is taken to be ~ 4.74 eV regardless of their sizes between ~ 2 to 10 nm, which is determined from the Kelvin probe analysis.[12] Similarly, the HOMO and LUMO positions and energy band-gap (E_g) of the GQD is calculated by directly converting the maximum emission wavelength (λ_{max}) into eV.[12] The HOMO and LUMO positions for our GQDs are found to be ~ 6.1 eV and ~ 3.3 eV respectively. In our GQD-LED system, electrons and holes are injected into luminescent GQDs by an external electrical bias through supporting electron transport layer (ZnO) and hole transport layer (Poly-TPD) respectively, and subsequently the recombination of charge carriers (electrons and holes) takes place within the GQDs.

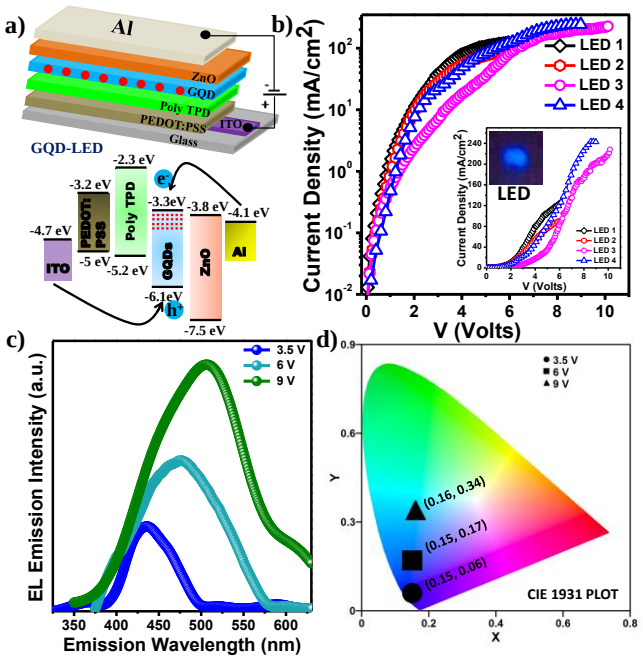

Figure 6. a) Schematic representation and electronic band diagram of the layer structured GQD-LED device, energy level values are taken from the literature.[33,34] b) Measured current density–voltage (J-V) characteristics of GQD-LED devices in logarithmic scale. Inset shows the current density in linear scale along with the true color photographic image of the GQD-LED device under operation. c) Bias dependent EL spectra of the GQD-LED devices. d) Calculated CIE chromaticity coordinates of the emissive color region from GQD-LEDs operated under different bias voltages. The bias voltages are shown in the inset.

Multiple devices are fabricated and characterized to check the reproducibility of GQD-LED device performances. The current density (J = I/A, where I is the current and A is the area of a device) as a function of the applied voltage (V) for different GQD-LED devices are shown in Figure 6b. Corresponding J-V curves for GQD-LEDs are represented in linear scale (inset of Figure 6b). The GQD-LED devices display the similar J-V characteristics with high current density. The true emission color of the GQD-LEDs is captured in photographic image (inset of Figure 6b). A blue emission is observed from the GQD-LED device under operation. Recently, organic synthesis of oleylamine capped GQD-OLED exhibiting white light emission was reported.[12] Similarly, water-soluble GQDs modified into organic medium by ex-situ functionalization with aniline showed blue PL emission and yellow color EL from aniline capped GQDs/MEH-PPV composite OLED with turn-on voltage of ~ 4 V have been reported.[22] While the turn-on voltage of the LED device containing PVK without GQDs is ~ 13 V, it decreases to ~ 8 V for the devices with composite of PVK:GQDs (3 wt%).[35] The existing reports to incorporate GQDs into LEDs involve the use of polymers in the composite form.[12,21,35] In contrary, our GQD-LED devices employ the pristine GQDs as active light emitting material. Importantly, a significant low turn-on voltage of ~ 2.5 V is obtained in comparison to the previous reports. We have prepared water-soluble GQDs, which was extracted into powder form without using any chemical modifications. The absence of bulky organic groups on the surface of emissive

GQDs presumably causes significantly low turn-on voltage by efficient charge carrier injection into GQDs at low voltages. Additionally, we have carried out control experiments to verify the EL appeared solely from the GQDs. We have designed a layered device structure similar to our GQD-LED devices except the emissive GQDs layer. Expectedly, the device doesn't show any EL behavior. To check the stability and reproducibility of the as prepared GQD-LED devices, the J-V measurements are carried out in ambient conditions (Figure S1, Supplementary Information). The device performances are comparable to vacuum sealed devices and exhibiting EL behavior in ambient condition.

The EL spectra obtained from GQD-LED devices under different bias voltages are shown in Figure 6c. The EL is found to be bias dependent showing a gradual red shift with increasing bias voltages. The observed trend is similar to the excitation wavelength dependent PL spectra, where a gradual transfer of carrier population towards longer wavelength PL band was observed with the excitation wavelengths. The corresponding Commission Internationale de l'éclairage (CIE) chromaticity coordinates diagram indicates bias dependent EL color from the GQD-LED (Figure 6d). The blue EL peak at ~ 436 nm observed at a low bias of 3.5 V (Figure 6c) and their corresponding CIE coordinates appears at (0.15, 0.06) (Figure 6d). With the increase in bias voltage to 6 V, the EL peak shifted to ~ 470 nm near cyan color. With the further increase in bias voltage to 9 V, a further red shift of the EL peak centered at ~ 500 nm with higher intensity was detected. Consistently, the CIE chromaticity diagram indicates that the corresponding EL color is shifted to deep cyan region. Hence, a change in color from blue to cyan can be obtainable with increasing bias voltages. The bias dependent EL spectra can be accounted from the existence of shallow defect levels just below the conduction band due to the amino-functionalization of GQDs, which resulted in the defect state PL apart from the intrinsic PL. The recombination of charge carriers takes place from both the intrinsic and defect states similar to the PL mechanism, however, excitation of specific energy states within the active emissive layer depends on the applied bias.[28] At low applied bias, charge carriers are injected into the intrinsic states

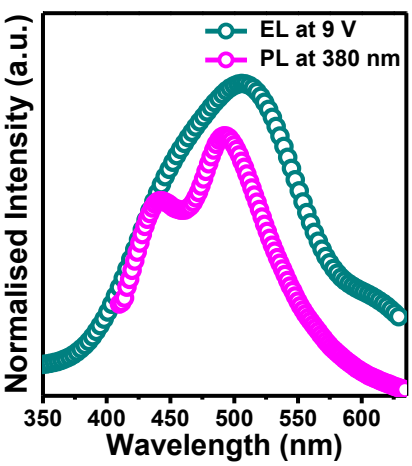

Figure 7. Comparison between EL spectrum of GQD-LED device operated at a bias voltage of ~ 9 V and PL spectrum of GQDs acquired at an excitation wavelength of ~ 380 nm.

with short life time ~ 6.6 ns (emission state at ~ 430 nm). At higher applied bias of 9V, the induced charge density into the GQD is increased and the charge carriers are injected into both intrinsic and defect states synchronously resulting in a significantly broad EL spectrum through multi-channel recombination processes. The EL from the as prepared GQD-LED devices traces the PL of GQDs (Figure 7 and see Figure S2a of Supplementary Information for CIE comparison). The close matching of the EL and PL spectra imply that the recombination of the charge carriers takes place within the GQDs demonstrating the successful fabrication of GQD-LED devices using water-soluble GQDs as active layer.

Conclusions

In summary, we reported for the first time a single step facile route to extract the water-soluble GQDs into powder form to fabricate LEDs. The powder-GQD samples were highly stable retaining the original intrinsic states. We have shown that the blue PL is dominated by the intrinsic state while defect sites play important roles in the low-energy cyan PL along with the intrinsic states. The GQD-LED devices exhibited a significantly low turn-on voltage of ~ 2.5 V, due to the absence of bulky organic groups on the surfaces of GQDs, which facilitates efficient charge carrier injection into the GQD layer. Additionally, the emissive light color is apparently bias-dependent and tunable color LED from the GQDs was successfully demonstrated. The charge carriers injected into GQDs was found to increase with the bias voltages leading to bias dependent color tunable EL from the GQD-LEDs. As of now, this is the only meaningful report on employing the exclusive emissive water-soluble GQDs as active layer in LEDs considering the large number of synthesis reports on water-soluble GQDs. We believe that the easy extraction route facilitate the preparation of thin films for optoelectronic device applications. GQD-LED devices operated in ambient conditions with significantly low driving voltages may found importance in solid-state lighting applications upon appropriate modifications.

Acknowledgements

Financial support from DST, India is gratefully acknowledged. G.S.K. and P.K.S. acknowledge DST INSPIRE fellowship.

Notes and references

Centre for Advanced Materials, Indian Association for the Cultivation of Science, Kolkata-700032, India.

Corresponding Author

* Email: camsa2@iacs.res.in

†Electronic Supplementary Information (ESI) available: [Additional Figures and information as described in the text]. See DOI: 10.1039/b000000x/

1 D. I. Son, B. W. Kwon, D. H. Park, W. S. Seo, Y. Yi, B. Angadi, C. L. Lee and W. K. Choi, *Nat. Nanotechnol*., 2012, **7**, 465.

2 Z. Wang, Y. Chen, P. Li, X. Hao, J. Liu, R. Huang and Y. Li, *ACS Nano*, 2011, **9**, 7149.

3 C. H. Lee, Y. J. Kim, Y. J. Hong, S. R. Jeon, S. Bae, B. H. Hong and G. C. Yi, *Adv. Mater*., 2011, **23**, 4614.

4 Y. S. Kim, K. Joo, S. K. Jerng, J. H. Lee, D. Moon, J. Kim, E. Yoon and S. H. Chun, *ACS Nano*, 2014, **8**, 2230.
5 J. Wu, M. Agrawal, H. A. Becerril, Z. Bao, Z. Liu, Y. Chen and P. Peumans, *ACS Nano*, 2010, **4**, 43.
6 C. O. Kim, S. W. Wang, S. Kim, D. H. Shin, S. S. Kang, J. M. Kim, C. W. Jang, J. H. Kim, K. W. Lee, S. H. Choi and E. Hwang, *Sci. Rep*., 2014, DOI:10.1038/srep05603.
7 J. Cai, C. A. Pignedoli, L. Talirz, P. Ruffieux, H. Sode, L. Liang, V. Meunier, R. Berger, R. Li, X. Feng, K. Müllen and R. Fasel, *Nat. Nanotechnol*., 2012, **9**, 896.
8 M. Bacon, S. J. Bradley and T. Nann, *Part. Part. Syst. Charact*., 2014, **31**, 415.
9 S. Zhu, J. Zhang, C. Qiao, S. Tang, Y. Li, W. Yuan, B. Li, L. Tian, F. Liu, R. Hu, H. Gao, H. Wei, H. Zhang, H. Sun and B. Yang, *Chem. Commun*., 2011, **47**, 6858.
10 S. Kim, S. W. Hwang, M. K. Kim, D. Y. Shin, D. H. Shin, C. O. Kim, S. B. Yang, J. H. Park, E. Hwang, S. H. Choi, G. Ko, S. Sim, C. Sone, H. J. Choi, S. Bae and B. H. Hong, *ACS Nano*, 2012, **6**, 8203.
11 H. Tetsuka, R. Asahi, A. Nagoya, K. Okamoto, I. Tajima, R. Ohta and A. Okamoto, *Adv. Mater*., 2012, **24**, 5333.
12 W. Kwon, Y. H. Kim, C. L. Lee, M. Lee, H. C. Choi, T. W. Lee and S. W. Rhee, *Nano Lett*., 2014, **14**, 1306.
13 L. A. Ponomarenko, F. Schedin, M. I. Katsnelson, R. Yang, E. W. Hill, K. S. Novoselov and A. K. Geim, *Science*, 2008, **320**, 356.
14 L. Tang, R. Ji, X. Cao, J. Lin, H. Jiang, X. Li, K. S. Teng, C. M. Luk, S. Zeng, J. Hao and S. P. Lau, *ACS Nano*, 2012, **6**, 5102.
15 M. Zhang, L. Bai, W. Shang, W. Xie, H. Ma, Y. Fu, D. Fang, H. Sun, L. Fan, M. Han, C. Liu and S. Yang, *J. Mater. Chem*., 2012, **22**, 7461.
16 D. Pan, J. Zhang, Z. Li and M. Wu, *Adv. Mater*., 2010, **22**, 734.
17 J. Peng, W. Gao, B. K. Gupta, Z. Liu, R. R. Aburto, L. Ge, L. Song, L. B. Alemany, X. Zhan, G. Gao, S. A. Vithayathil, B. A. Kaipparettu, A. A. Marti, T. Hayashi, J. J. Zhu and P. M. Ajayan, *Nano Lett*., 2012, **12**, 844.
18 J. Lu, P. S. E. Yeo, C. K. Gan, P. Wu and K. P. Loh, *Nat. Nanotechnol*., 2011, **6**, 247.
19 Z. Zhang and P. Wu, *Cryst. Eng. Comm*., 2012, **14**, 7149.
20 J. Shen, Y. Zhu, X. Yang, J. Zong, J. Zhang and C. Li, *New J. Chem*., 2012, **36**, 97.
21 V. Gupta, N. Chaudhary, R. Srivastava, G. D. Sharma, R. Bhardwaj and S. Chand, *J. Am. Chem. Soc*., 2011, **133**, 9960.
22 B. X. Zhang, H. Gao and X. L. Li, *New J. Chem*., 2014, **38**, 4615.
23 C. M. Luk, L. B. Tang, W. F. Zhang, S. F. Yu, K. S. Teng, S. P. Lau, *J. Mater. Chem*., 2012, **22**, 22378.
24 W. S. Hummers and R. E. Offeman, *J. Am. Chem. Soc*., 1958, **80**, 1339.
25 A. K. Geim and K. S. Novoselov, *Nat. Mater*., 2007, **6**, 183.
26 A. W. Robertson and J. H. Warner, *Nanoscale*, 2013, **5**, 4079.
27 K. W. Urban, *Nat. Mater*., 2011, **10**, 165.
28 X. Zhang, Y. Zhang, Y. Wang, S. Kalytchuk, S. V. Kershaw, Y. Wang, P. Wang, T. Zhang, Y. Zhao, H. Zhang, T. Cui, Y. Wang, J. Zhao, W. W. Yu and A. L. Rogach, *ACS Nano*, 2013, **7**, 11234.
29 X. Li, S. P. Lau, L. Tang, R. Ji and P. Yang, *J. Mater. Chem. C*, 2013, 1, 7308.
30 G. S. Kumar, R. Roy, D. Sen, U. K. Ghorai, R. Thapa, N. Mazumder, S. Saha and K. K. Chattopadhyay, *Nanoscale*, 2014, **6**, 3384.
31 S. Zhu, Y. Song, X. Zhao, J. Shao, J. Zhang and B. Yang, *Nano Res*., 2014, DOI: 10.1007/s12274-014-0644-3.
32 S. Chen, X. Hai, C. Xia, X. W. Chen and J. H. Wang, *Chem. Eur. J*., 2013, **19**, 15918.
33 X. Yang, D. Zhao, K. S. Leck, S. T. Tan, Y. X. Tang, J. Zhao, H. V. Demir and X. W. Sun, *Adv. Mater*., 2012, **24**, 4180.
34 B. S. Mashford, M. Stevenson, Z. Popovic, C. Hamilton, Z. Zhou, C. Breen, J. Steckel, V. Bulovic, M. Bawendi, S. C. Sullivan and P. T. Kazlas, *Nat. Photonics*, 2013, **7**, 407.
35 S. H. Song, M. H. Jang, J. Chung, S. H. Jin, B. H. Kim, S. H. Hur, S. Yoo, Y. H. Cho and S. Jeon, *Adv. Optical Mater*., 2014, **2**, 1016.

Table of Contents

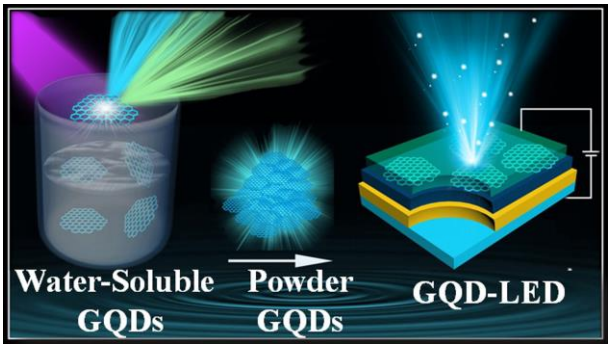

Graphene quantum dots in powder form obtained in single-step leads fabricating color tunable light emitting diodes with low turn-on voltages.